Int. J. Electrochem. Sci., 14 **(2019)** 11110 – 11121, doi: 10.20964/2019.12.77

International Journal of ELECTROCHEMICAL SCIENCE
www.electrochemsci.org

Experimental and Theoretical Studies of (2R)-5-hydroxy-7-methoxy-2-phenyl-2,3-dihydrochromen-4-one as corrosion inhibitor for Iron in Hydrochloric Acid

Saprizal Hadisaputra[1*], *Agus Abhi Purwoko*[1], *Rahmawati*[1], *Dina Asnawati*[2], *Ilhamsyah*[2]
Saprini Hamdiani[2], *Nuryono*[3]

[1] Chemistry Education Division, University of Mataram, Jalan Majapahit No 62, Mataram, 83125, Indonesia.
[2] Department of Chemistry, University of Mataram. Jalan Majapahit 62, Mataram, 83125, Indonesia
[3] Department of Chemistry, Universitas Gadjah Mada, Sekip Utara, Yogyakarta 55281, Indonesia
[*]E-mail: rizal@unram.ac.id

Received: 19 July 2018/ *Accepted:* 14 May 2019 / *Published:* 29 October 2019

The corrosion inhibition on the iron surfaces by (2R)-5-hydroxy-7-methoxy-2-phenyl-2,3-dihydrochromen-4-one (PN), isolated from *Kaempferia pandurata Roxb*, has been conducted both experimentally and theoretically. The corrosion inhibition effectiveness of PN was studied by gravimetric and electrochemical experiments and density function calculation at B3LYP level of theory. The PN successful isolation was confirmed by spectroscopic techniques.The presence of an inhibitor can effectively inhibit iron corrosion in 1M HCl. The adsorption of PN on the iron surface obeyed the Temkin adsorption and physisorption mechanism. The effect of electron donating and withdrawing groups on the inhibition efficiency was studied by density functional theory method. The inhibition efficiency of PN increased with the addition of the N-NH_2 function group whereas the NO_2 group gave the opposite result.

Keywords: acidic inhibitor, iron, gravimetric, EIS, DFT.

1. INTRODUCTION

In the search for eco-friendly, inexpensive and efficient corrosion inhibitor, the natural product compounds become an important solution. Extract of natural products for inhibiting corrosion have been widely reported and they showed high corrosion inhibition efficiency [1-8]. They generally utilize their heteroatom groups and π electron to interact with metal for inhibiting corrosion processes [9]. The interaction process forms a coating on the metal surfaces, thus protecting the metal in the corrosive medium [10]. However, the extracts were still a mixture of various compounds; it leads to the difficulty of detecting compounds that play the most significant role as corrosion inhibitors. Furthermore, the plant extracts inhibition efficiencies are still dependent on the plant part and location.

To overcome these uncertainties and dependencies, it is necessary to isolate the pure compounds from the targeted plants. Therefore, in this work the (2R)-5-hydroxy-7-methoxy-2-phenyl-2,3-dihydrochromen-4-one (PN) was crystalized to 99.99 % purity from *Kaempferia pandurata Roxb* extract and tested as a corrosion inhibitor.

Kaempferia pandurata Roxb or finggerroot plant can be found easily in Indonesia and Southeast Asia region. It is commonly used as a spice cooking and as a traditional medicine for colds, asthma, stomach ache, and headaches. PN compound is the major compound of *Kaempferia pandurata Roxb*. The PN structure has two benzene rings and the presence of π electron donors from aromatic benzene and electrophilic properties of heteroatoms enables the compound to be strongly bonded to the metal surface. Such a structure allows high-potential PN as a corrosion inhibitor. In this work, PN was isolated using simple soxhletation techniques, purified, characterized and tested for corrosion inhibition properties using weight loss measurement and electrochemical analysis. A theoretical study was then used to explain the relationship between the molecule electronic parameters and their corrosion inhibition performance.

2. MATERIAL AND METHOD

2.1. Materials

All chemicals are ordered from Sigma Aldrich/Indonesia. Fourier transform infrared (FTIR) spectra were obtained by a Shimadzu FTIR-8300 spectrometer. Nuclear magnetic resonance spectra were recorded on ^{1}H NMR 500Hz JEOL Spectroscopy. Gas Chromatography-Mass Spectroscopy GC-MS QP2010 shimadzu was also used.

2.2. Extraction

Isolation was performed using a simple soxhletation technique. Dry powder of *Kaempferia pandurata Roxb* was extracted using n-hexane by soxhlet extraction technique. The soxhlet result was then evaporated to obtain the filtrate using a vacuum rotary evaporator. The filtrate was then cooled to 2 °C overnight until PN crystals are formed. The formed crystals were then purified by recrystallization technique with 92 % yield. White PN crystals are formed with a melting point of 99.5 ^{o}C. Characterization was then performed using FTIR, ^{1}H NMR and GC-MS. FTIR spectrum: OH group 3437.46 cm^{-1}; C=O keton group 1645.43 cm^{-1}; C-O 1250 and 1290 cm^{-1}; C=C aryl aromatic 1622.26-1579.64 cm^{-1}; C-H methyl and methylen aliphatic 3000-2800 cm^{-1} and 1450-1350 cm^{-1}; C-O aryl 1290 and 1250 cm^{-1}. ^{1}H-NMR spectra: 3.75 ppmfor 3Hsinglet of $ArOCH_3$; 6.019 ppm for 2H singlet; 11.948 ppm for 1H of OH singlet; 2.817-3.029 ppm for 2H cis and trans multiplet; 5.284 ppm for 5H doublet. Molecular weight = 270 g.mol^{-1}.

2.3. Corrosion test

The iron specimens were made with an effective area of 1 cm^2, and iron sample was suspended in 100 mL of 1 M HCl solution with or without an inhibitor. The studied inhibitor concentrations were

7.27×10^{-4} M, 9.69×10^{-4} M, 1.21×10^{-3} M and 1.45×10^{-3} M. After 1, 2, 3, 4, 12, 24 and 48 hours, the sample was washed, dried, and weighed. All weight loss measurement was repeated three times to obtain the average result for comparison. The inhibition efficiencies (IE%) were calculated using Eq. 1.

$$IE\% = \left(1 - \frac{w_2}{w_1}\right) \times 100\%$$

where W1 and W2 are the lost weight of the iron specimen in the absence and presence of an inhibitor, respectively.

2.4 Electrochemical Impedance Measurements

The surface preparation of the iron electrode was conducted by silica carbide paper 800 and 2000 grid, and re-washed using distilled water and ethanol before use. Furthermore, the electrodes are connected with a potentiostat PG 301. The 1 M HCl solutions were prepared from 6 M HCl and distilled water. Addition of inhibitor solution was carried out on various concentrations of7.27×10–4 M, 9.69×10–4 M, 1.21×10–3 M and 1.45×10–3 M at 298 K, 308 K and 318 K.The analysis begins with the EIS potential open circuit measurement at a frequency of10 kHz – 100 mHz.

2.5. Computational details

The density functional theory at B3LYP/6-31G(d) method is used to optimize PN geometry. Hence corrosion predominantly occurs in the aqueous medium, so the polarized continuum model was used to calculate the solvent effects. Because it has a little effect on the energetic, only single-point calculation was applied in aqueous phase [11-14]. All theoretical calculations are performed with the Gaussian 03 package [15]. The electronic parameters HOMO and LUMO energy, gap energy (Egap), the absolute electronegativity (χ), the fraction of electron transferred (ΔN), and the theoretical corrosion inhibition efficiency (IE%) were calculated [16-18].

3. RESULTS AND DISCUSSION

3.1. Isolation and characterization

Isolation of PN compound (Figure 1) produces white crystal with *Kaempferia pandurata Roxb* typical aroma with a yield of 92 %. The crystals were then identified using thin layer chromatography (TLC). The retention factor value of the TLC sample is equal to the standard retention factor value of 0.750. The crystal has a melting point of 98 °C. This result is in accordance with experimental studies melting point tests for PN compound [20]. To strengthen the identification results, further analysis was performed using FTIR, ^{1}H NMR and GC-MS. Identification by FTIR spectroscopy identifies wavelengths of 3437.46 cm^{-1} of OH binding to C=O; 3061.30 cm^{-1} denotes CH aromatics; C=O of the ketone is indicated by the wavelength 1645.40 cm^{-1}; 1622.25 cm^{-1} and 1579.64 cm^{-1} identification for aromatic; the methyl and methylene groups were indicated in3000-2800 cm^{-1}and1450-1350 cm^{-1}, respectively; the presence of the C-O group were identified at 1250-1290 cm^{-1}.

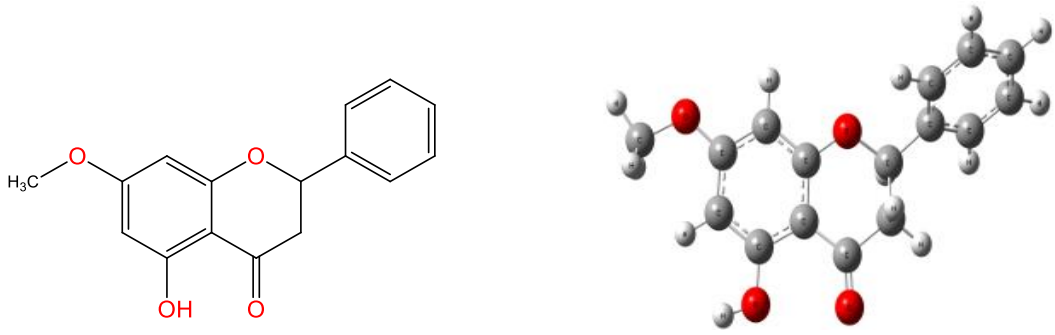

Figure 1. The structure of 5-hydroxy-7-methoxy-2-phenylchroman-4-one and the optimized structures of PN molecule determined using DFT method.

The ^{1}H NMR indicate a chemical shift of 3.75 ppm singlet showing 3 hydrogen from the $ArOCH_3$ group; 6.019 ppm singlet also shows 2 hydrogen at 6 and 8 positions; 11.948 ppm return singlet denotes one hydrogen in the OH group; 2.817-3.029 ppm multiplet identifies the presence of 2 hydrogen in cis or trans positions, multiplets in this case because of the overlap and different coupling concealments of H in cis or trans positions; 5.284 ppm doublet represents one hydrogen in position 2. The GC-MS shows the relative molecular weight of the PN compound is m/z = 270 with fragmentation of m/z = 77; 123; 193; 252; 242,227, 213. The GC-MS characterization data confirm that the isolated compound was PN with 99.99 % purity.

3.3. Weight loss studies

The inhibition efficiencies of PN were calculated using weight loss measurements at different concentrations as depicted Figure 2**.** Corrosion inhibition efficiencies increase with increasing concentration of inhibitor, in contrast reducing inhibitor concentration decreasesthe inhibition efficiencies. The efficiency of inhibition reached a maximum efficiency at 298 K and 1.1 x 10^{-3} M. It indicates that the PN are able to protect iron surface from corrosion. The PN has free electron donors from oxygen and aromatic benzene rings that donate π electrons to the formation of physisorption on the iron surfaces.

The effect of temperature on corrosion inhibition efficiency can also be seen in Figure 2. Experiments of corrosion inhibition efficiency were carried out at different temperatures (298 K, 308 K, and 318 K) to measure the effect of temperature changes on the efficiency of corrosion inhibition. Increasing inhibitor concentration and decreasing temperature result in increased performance inhibition. This can be explained from the exothermic inhibition process, the heat value of adsorption is negative, which means an increase in corrosion inhibition efficiency when the temperature decreases [22,23]. The gravimetric results showed good agreement with the results of EIS measurements.

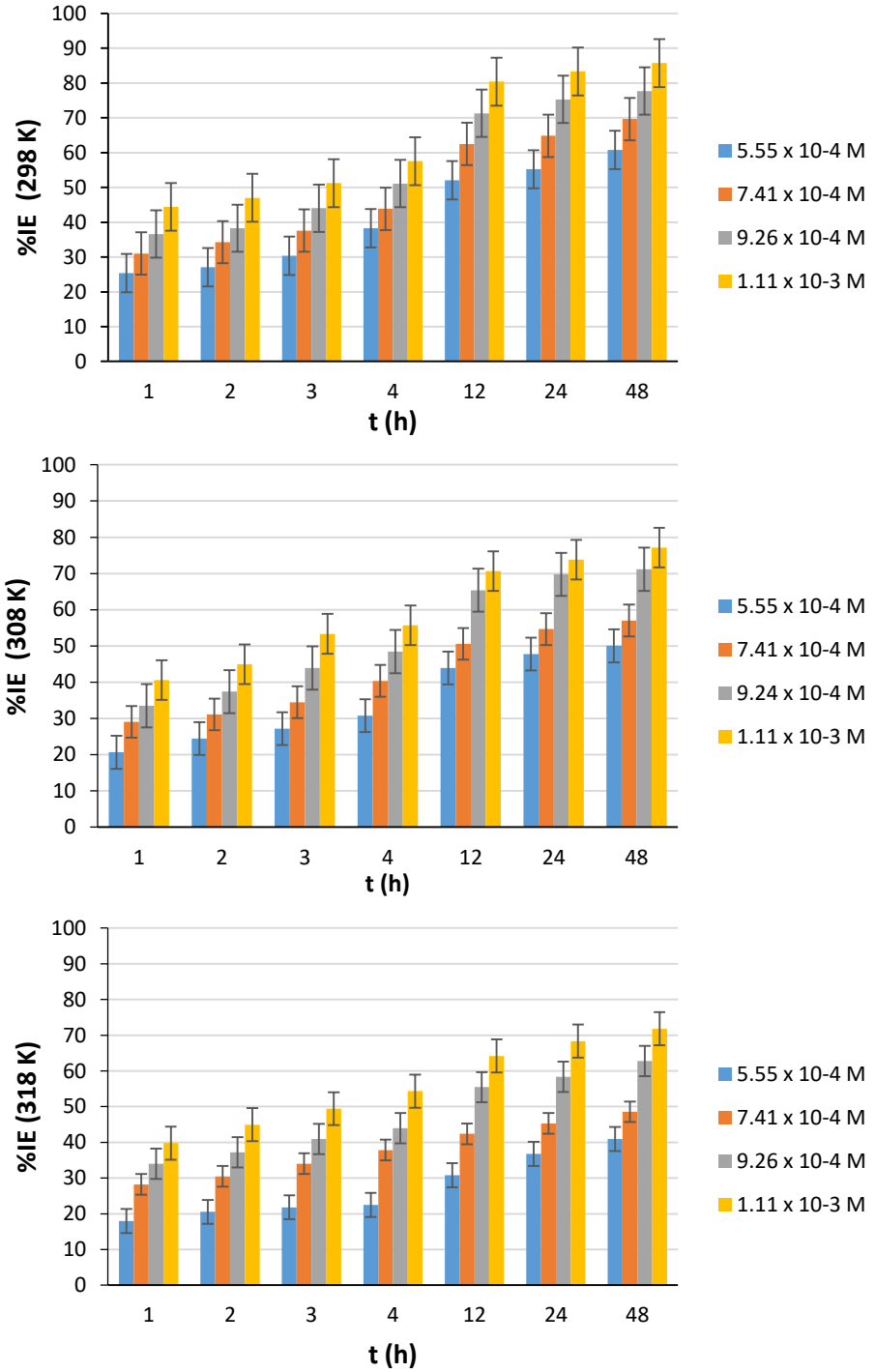

Figure 2. Weight loss studies of inhibition efficiency of PN for iron at 1 M HCl as a fuction of time at various inhibitor concentrations (5.55×10^{-4} M, 7.41×10^{-4} M, 9.26×10^{-3} M and 1.11×10^{-3} M) and temperatures (298 K, 308 K, and 318 K).

3.3 Electrochemical impedance spectroscopy (EIS)

The EIS test results show the Nyquist curve in the form of a semicircular diagram which is a plot of real impedance (Zr) against imaginary impedance (-Zi). The electrical (electrochemical) parameters produced are Rct, Rs, and Cdl obtained based on data fittings. Rct is a charge transfer resistance formed by a single electrochemical reaction on a metal surface controlled by kinetics. Rs is

the solution resistance which is influenced by ion concentration, ion type, and geometry of the current carrying area, while Cdl is the electric double layer capacitance formed from ions attached to the electrode surface. The inhibitor efficiency value is calculated by the following equation:

$$\%IE = \left\{\frac{Rct\ (inh) - Rct\ (blank)}{Rct\ (inh)}\right\} \times 100$$

where, Rct (inh) and Rct (blank), respectively, are obstacles to transfer of charge with and without the PN compound being tested.

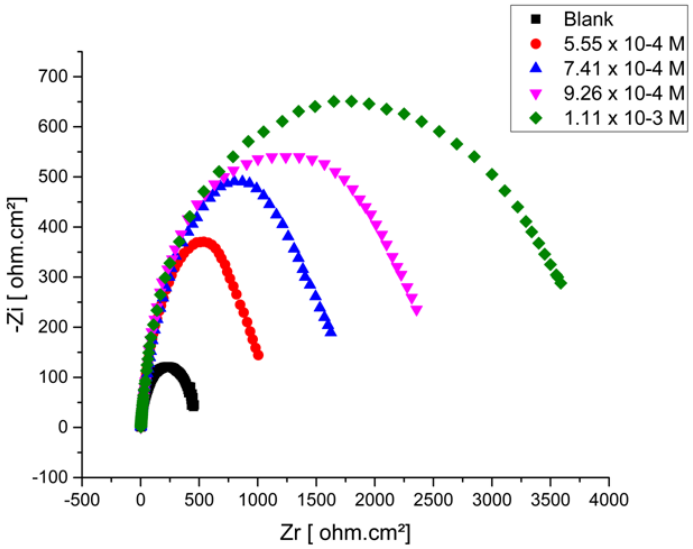

Figure 3. Nyquist diagrams at temperature (298 K) and various concentration of PN (5.55×10^{-4} M, 7.41×10^{-4} M,9.26×10^{-4} M and 1.11×10^{-3} M).

Figure 3 shows the Nyquist curve for iron plate in corrosive media (1 M HCl) from the efficiency testing of inhibitors of PN at various concentrations. The half circle in the Nyquist curve looks imperfect which shows that the metal surface is not homogeneous [23]. The addition of PN inhibitor increase the resistance of charge transfer resistance (Rct). This shows that the addition of inhibitor inhibit the transfer of electrons from the iron surface to the solution medium so that the iron oxidation reaction and the reduction of ions in the solution decrease. The inhibitor has the ability to inhibit corrosion as indicated by enlarging the semicircular curve on the Nyquist curve along with the addition of inhibitor concentrations [24].

Table 1 shows the electrochemical parameters in the form of charge transfer resistance (Rct), solution resistance (Rs), and double layer capacitance (Cdl), and the efficiency of PN inhibitor corrosion inhibitor efficiency. The addition of inhibitor concentrations of PN compounds from 5.55 x 10^{-4} M to 1.11 x 10^{-3} M increased the barriers to maximum charge transfer (Rct) by 3587.8 Ω cm^2 compare with blank solution. The formation of protective film on metal surfaces is indicated by increasing Rct values due to the addition of inhibitor concentrations. Simultaneously there was a decrease in Cdl value which indicated the occurrence of PN adsorption on metal surfaces [24,25].

Table 1. Impedance parameters for iron in 1 M HCl solution with and without different concentrations of the investigated inhibitors at 298 K, 308 K and 318 K

T (K)	C (M)	R_s (Ω cm^2)	R_{ct} (Ω cm^2)	C_{dl} (μFcm^{-2})	f(Hz)	θ	%IE
298	Blank	2.653	440.2	253.41	1.43	-	-
	5.55 x 10^{-4}	2.874	1005.6	79.76	1.99	0.5623	56.2251
	7.41 x 10^{-4}	2.435	1624.6	64.52	1.52	0.7290	72.9041
	9.26 x 10^{-4}	2.319	2356.4	53.83	1.26	0.8132	81.3189
	1.11 x 10^{-3}	2.206	3587.8	39.439	1.13	0.8377	84.9706
308	Blank	1.974	112.7	123.35	1.15	-	-
	5.55 x 10^{-4}	2.416	243.2	64.42	1.02	0.5366	53.6595
	7.41 x 10^{-4}	2.285	289.5	52.94	1.04	0.6107	61.0708
	9.26 x 10^{-4}	2.195	420.0	35.54	1.07	0.7317	73.1667
	1.11 x 10^{-3}	1.857	550.7	24.06	1.20	0.7953	79.5351
318	Blank	2.084	34.0	237.57	1.97	-	-
	5.55 x 10^{-4}	2.164	60.1	85.44	3.10	0.4343	43.4276
	7.41 x 10^{-4}	1.958	70.4	70.25	3.22	0.5170	51.7045
	9.26 x 10^{-4}	1.785	96.5	64.63	2.55	0.6477	64.7668
	1.11 x 10^{-3}	1.698	134.2	54.35	2.18	0.7466	74.6647

3.3. Adsorption Thermodynamics

Thermodynamic factors such as activation energy, enthalpy and entropy changes, and adsorption-free energy can be used to determine the inhibition process. Activation energy (Ea) is the minimum energy required for the ongoing chemical reaction. Ea value indicates that the higher the concentration the greater the activation energy required. The greater Ea value indicates a greater energy barrier to inhibit the oxidation reaction in the corrosion process. The bigger the Ea value the smaller the corrosion rate. The Ea value < 80 kJ indicates the occurrence of physical adsorption while the value of Ea > 80 kJ indicates the occurrence of chemical adsorption [26]. It was found that the Ea values were 10.80 kJ.mol^{-1}, 15.42 kJ.mol^{-1}, 25.92 kJ.mol^{-1} and 36.92 kJ.mol^{-1} at 5.55 x 10^{-4} M, 7.41 x 10^{-4} M, 9.26 x 10^{-4} M and 1.11 x 10^{-3} M, respectively. It means that the adsorption of PN on Iron surface featuring physisorption mechanism.

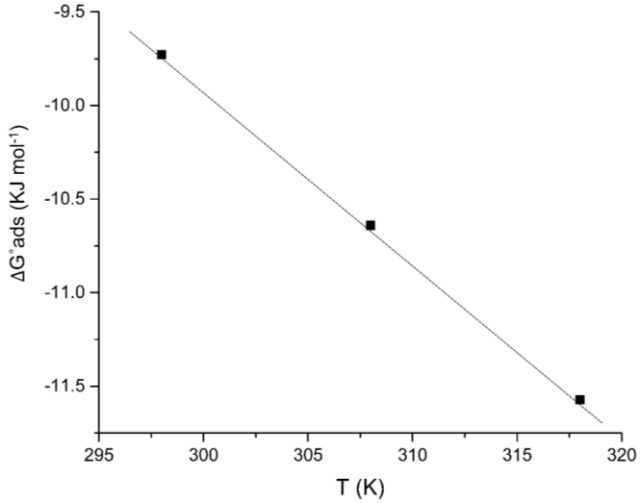

Figure 4. The relationship between ΔG_{ads}^{o} and $T$for PN in 1 M HCl solution.

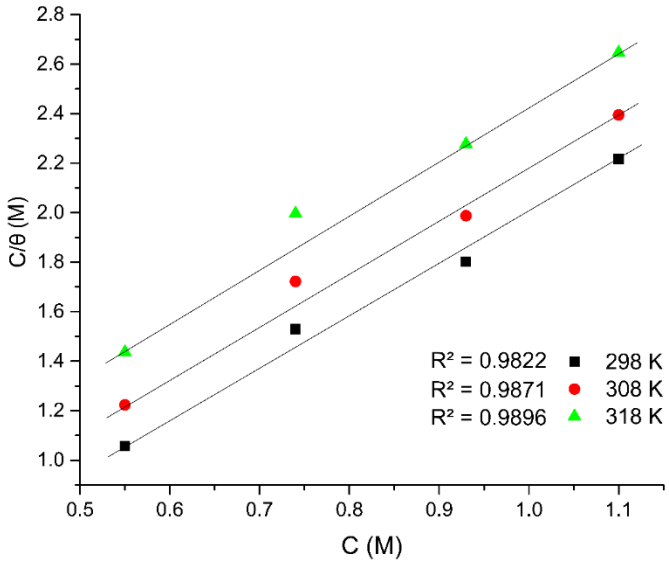

Figure 2. Temkin adsorption isotherm of PN on iron surfaces in 1 M HCl at different temperatures

The higher the enthalpy value the more difficult the corrosion occurs because it requires greater energy. In this study the value of enthalpy increases as the temperature increases. The enthalpy values for the temperature of 5.55 x 10^{-4} M, 7.41 x 10^{-4} M, 9.26 x 10^{-4} M and 1.11 x 10^{-3} M were 51.78 kJ.mol^{-1}, 62.45 kJ.mol^{-1}, 65.90 kJ.mol^{-1} and 73.74 kJ.mol^{-1}, respectively. The value of the enthalpy was positive indicate that corrosion procession was endothermic at the presence of inhibitor. However, the value of entropy increases as the concentration increases: 0.292 kJ.mol^{-1}, 0.373 kJ.mol^{-1}, 0.388 kJ.mol^{-1}.K^{-1} and 0.461 kJ.mol^{-1}.K^{-1} respectively. The value of the adsorption entropy was also positive, meaning that the adsorption occurs spontaneously.

Information on the interaction mechanism between inhibitor and metal surfaces is obtained from isothermal adsorption. The surface coverage value (θ) of PN at various concentrations has been tested according to the best isothermal conditions. Plot θ vs ln C at different temperatures gives a straight line as shown in Figure 2. Thus, the best fit is obtained from Temkin adsorption. Isothermal Temkin identifies that PN adsorption on Iron surfaces is multilayer and more likely to be physisorption. The physisorption adsorption process is also indicated by the value of ΔG^{o}_{ads}< -20 kJ.mol^{-1}.

3.4. Density functional theory calculation

In this work, theoretical calculations are used to predict PN derivatives with higher inhibition efficiency. Here, we tested three potential PN derivatives as corrosion inhibitors 6-amino-5-hydroxy-7-methoxy-2-phenylchroman-4-one (PN-NH_2), 6-diazenyl-5-hydroxy-7-methoxy-2-phenylchroman-4-one (PN-NNH_2) and 5-hydroxy-7-methoxy-6-nitro-2-phenylchroman-4-one (PN-NO_2). Structure of the studied molecules is depicted in Figure 3. Table 3 shows the parameters of quantum descriptor, corrosion inhibition efficiencies and binding energies of the PN and its derivatives.

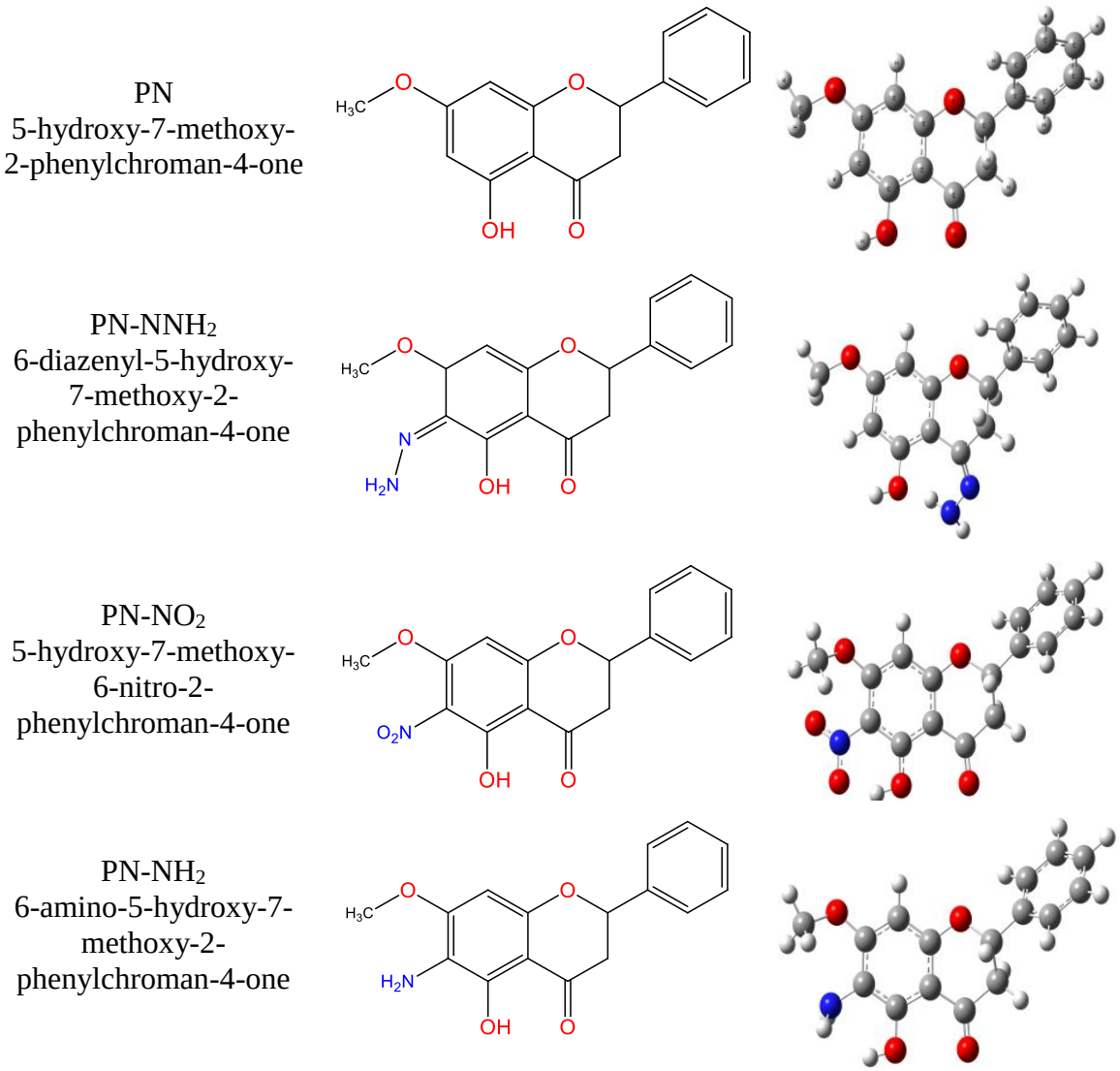

Figure 3. 2D and optimized structures of PN and its derivatives

Corrosion inhibition efficiency depends not only on the molecular structure parameters but also depends on the condition of the molecular electronic parameters. Reactivity of inhibitors can be measured by the value of electronic parameters such as theHOMO and LUMO energies.The interaction between EHOMO and ELUMO leads to electron transition within molecules [27,28] and it can be measured based on the values of molecular orbital energy. The tendency of molecules to donate electrons can be seen from the energy value of HOMO. The HOMO energies indicate that PN-NNH_2 has higher HOMO energy than PN, PN-NH_2 and PN-NO_2. Therefore, PN-NNH_2 is more intent on donating electrons to iron than PN, PN-NH_2 and PN-NO_2. This trend explains why PN-NNH_2 has the highest inhibition efficiency.

Tabel 2. The quantum chemical parameters, corrosion inhibition efficiencies and binding energies of the PN and its derivatives obtained from DFT/B3LYP/6-31G(d) level of theory.

	E_{HOMO} eV	E_{LUMO} eV	E_{gap} eV	χ eV	ΔN	IEtheor.%	ΔEb (kcal.mol^{-1})
PN	-6.24	-1.51	4.72	3.88	0.65	84.97	-51.50
PN-NH_2	-6.13	-1.53	4.59	3.83	0.68	85.79	-53.71
PN-NO_2	-6.25	-1.24	5.01	3.75	0.64	84.34	-33.24
PN-NNH_2	-5.57	-0.76	4.81	3.16	0.79	89.31	-55.08

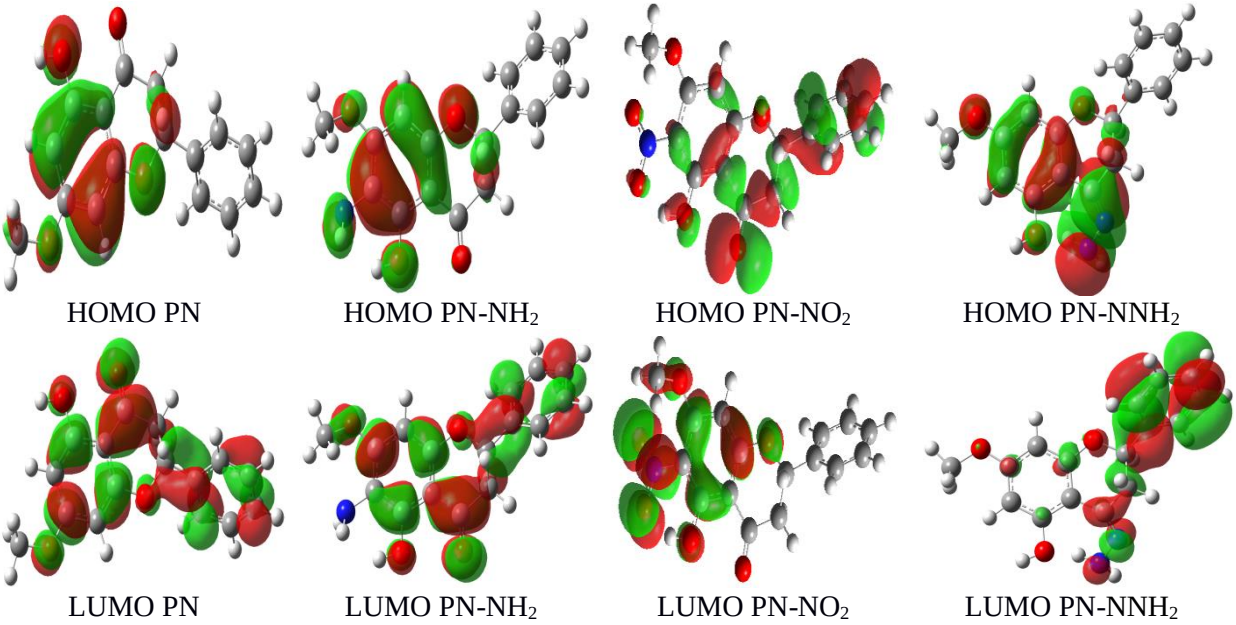

Figure 4. HOMOs and LUMOs of PN and its derivatives obtained with DFT/B3LYP/6-31G(d) level of theory.

Electronegativity indicates the level of stability of the molecule. A small electronegativity value causes the molecule to easily achieve stability [27,28]. Table 2 shows the smallest electronegativity was shown by PN-NNH_2. The electronegativity value of PN-NNH_2 is 3.16eV, this value is lower than PN, PN-NH2, PN-NO_2 with 3.88 eV, 3.83 eV and 3.75 eV, respectively. This electronegativity shows that the PN has the highest stability, thus it is predicted that PN- NNH_2 has the highest inhibition efficiency.

Table 2 presents the number of electrons transferred (ΔN). If the ΔN value is smaller than 3.6, it can be concluded that the inhibition efficiency increases due dilution of electrons to the metal surface [29]. The higher the value of electrons transferred number, the higher the ability of the inhibitors to donate their electrons toward the metal surface. The PN-NNH_2shows the highest fraction of electrons transferred and it is associated with the highest inhibition efficiency. In contrast, PN-NO_2indicates the opposite process.

Theoretical prediction of corrosion inhibition efficiency (IETheor.%) of PN and its derivatives is also depicted in Table 2. The addition of substitution groups to PN affects the efficiency of corrosion inhibition. The corrosion inhibition of PN and derivatives are sorted as follows: PN-NO_2< PN < PN-NH_2< PN-NNH_2. The sequence of efficiency of this corrosion inhibitor correlates linearly with quantum chemical parameter values. The addition of substitution groups has an effect on the efficiency of corrosion inhibition due to differences in electron distribution in studied molecules as shown in Figure 4. In PN-NNH_2 the nucleophile difference is centered on NNH_2 and in PN-NO_2 centered only on OH group. Therefore, the inhibitor PN-NNH_2 is likely to bind strongly toward the surface of iron than that of PN-NO_2 so that it has better inhibition performance.

The binding energy (ΔEb) values show that interaction between PN and iron formed stable complexes (Table 2). The more negative the interaction energy is, the more stable the complex. The order of complex stability between PN and its derivatives with iron is PN-NNH_2 > PN-NH_2 > PN > PN-NO_2. The value of the binding energy is in good correlation with the predicted corrosion inhibition efficiency. The addition of electron donor NNH_2 and NH_2 groups increases the complex stability; as a result, the inhibition efficiency of the inhibitor is also increased.

4. CONCLUSION

The experimental and theoretical studies of PN as corrosion inhibitors of Iron in 1 M HCl have been performed. The FTIR spectra, ^{1}H NMR and GC-MS characterized the successful isolation of PN from *Kaempferia pandurata Roxb*. The 84.97 % inhibition efficiency was obtained at maximum PN concentration. Isothermal adsorption obeys the Temkin adsorption multilayer featuring physisorption mechanism.The efficiency of corrosion inhibition of PN and its derivatives correlates well with quantum electronic parameters such as the frontier molecular orbital, gap energy, electronegativity, and electron transfer as well as binding energy. The addition of the NNH_2 group within the framework of PN increased the efficiency of corrosion inhibition by 5 %.

ACKNOWLEDGEMENTS
This research obtained funding from KEMENRISTEKDIKTI Indonesia, Grant Number 1841/UN18.L1/PP/2018, and their support is gratefully acknowledged.

References

1. P.E. Alvarez, M.V. Fiori-Bimbi, A. Neske and S.A. Brandán and C.A. Gervasi, *J. Ind. Eng. Chem.*, 58 (2018) 92-99.
2. C. Verma, M.A. Quraishi, E.E. Ebenso and I. Bahadur, *J. Bio. Tribo. Corros.*, 4 (2018) 3 33.
3. Y. Qiang, S. Zhang, B. Tan and S. Chen, *Corros. Sci.*, 133 (2018) 6-16.
4. S. Hadisaputra, A.A. Purwoko, I. Ilhamsyah, S. Hamdiani, D. Suhendra, N. Nuryono, and B. Bundjali, *Int. J. Corros. Scale. Inhib.*, 7 (2018) 4 633-647.
5. F.E.T. Heakal, M.A. Deyab, M.M. Osman and A.E. Elkholy, *Desalination*, 425 (2018) 111-122.
6. M. Srivastava, P. Tiwari, S. Srivastava, A. Kumar, G. Ji and R. Prakash, *J. Mol. Liq.*, 254 (2018) 357-368.
7. G. Ji, S. Anjum, S. Sundaram and R. Prakash, *Corros. Sci.*, 9 (2015) 107-117.

8. P.C. Okafor, E.E. Ebenso and U.J. Ekpe, *Int. J. Electrochem. Sci.*, 5 (2010) 978 – 993
9. Z. Salarvand, M. Amirnasr, M. Talebian, K. Raeissi and S. Meghdadi, *Corros. Sci*., 114, (2017) 133–145
10. R. Solmaz, G. Kardaş, M. Culha, B. Yazıcı and M. Erbil, *Electrochim. Acta*, *53* (2008) 20 5941-5952.
11. S. Hadisaputra, L.R. Canaval, H.D. Pranowo and R. Armunanto, *Monatsh. Chem*., 145 (2014) 5 737-745.
12. S. Hadisaputra, L.R. Canaval, H.D. Pranowo and R. Armunanto, *Indones. J. Chem.*, 14 (2014) 2 199-208.
13. S. Hadisaputra, H.D. Pranowo and R. Armunanto, *Indones. J. Chem*., 12 (2012) 3 207-216.
14. S. Hamdiani, I.H. Rohimah, Nuryono, A.A. Purwoko, L.R.T. Savalas and S. Hadisaputra, *Asian J. Chem.*, 31 (2019) 2 303-308
15. M.J. Frisch, G.W. Trucks, H.B. Schlegel, G.E. Scuseria, M.A. Robb, J.R. Cheeseman, J.A. Montgomery, T.J. Vreven, K.N. Kudin, J.C. Burant, J.M. Millam, S.S. Iyengar, J. Tomasi, V. Barone, B. Mennucci, M. Cossi, G. Scalmani, N. Rega, G.A. Petersson, H. Nakatsuji, M. Hada, M. Ehara, K. Toyota, R. Fukuda, J. Hasegawa, M. Ishida, T. Nakajima, Y. Honda, O. Kitao, H. Nakai, M. Klene, X. Li, J.E. Knox, H.P. Hratchian, J.B. Cross, C. Adamo, J. Jaramillo, R. Gomperts, R.E. Stratmann, O. Yazyev, A.J. Austin, R. Cammi, C. Pomelli, J.W. Ochterski, P.Y. Ayala, K. Morokuma, G.A. Voth, P. Salvador, J.J. Dannenberg, V.G. Zakrzewski, S. Dapprich, A.D. Daniels,M.C. Strain, O. Farkas, D.K. Malick, A.D. Rabuck, K. Raghavachari, J.B. Foresman, J.V. Ortiz, Q. Cui, A.G. Baboul, S. Clifford, J. Cioslowski, B.B. Stefanov, G. Liu, A. Liashenko, P. Piskorz, I. Komaromi, R.L. Martin, D.J. Fox, T. Keith, M.A. Al-Laham, C.Y. Peng, A. Nanayakkara, M. Challacombe, P.M.W. Gill, B. Johnson, W. Chen, M.W. Wong, C. Gonzalez, J.A. Pople, Gaussian03, Gaussian, Inc.,Pittsburgh, PA, 2003.
16. S. Hadisaputra, S. Hamdiani, M.A. Kurniawan and N. Nuryono, *Indones. J. Chem.*, 17 (2017) 3 431-438.
17. R. Obayes, A. Al-Amiery, G. Alwan, A. Alobaidy, A. Al-Amiery, A. Kadhum and A. Mohamad, *Chem. Cent. J.*, 8 (2014) 21 1–8
18. R. Obayes, A. Al-Amiery, G. Alwan, A. Alobaidy, A. Al-Amiery, A. Kadhum and A. Mohamad, *J. Mol. Struct.*, 1138 (2017) 27–34
19. S.K. Shukla and E.E. Ebenso, *Int. J. Electrochem. Sci.*, 6 (2011) 3277
20. A.Y.L. Ching, T. S. Wah, M.A. Sukari, G.E.C Lian, M. Rahmani and K. Khalid. *Malaysian J. Anal. Sci.*, 11 (2007) 1 154-159.
21. A. Zarrouk, I. Warad, B. Hammouti, A. Dafali, S.S. Al-Deyab and N. Benchat, *Int. J. Electrochem. Sci*, *5* (2010) 10 1516-26.
22. N.I. Kairi, J. Kassim, *Int. J. Electrochem. Sci.*, *8*, (2013) 7138-7155.
23. S.K. Shukla, M.A. Quraishi, *Corros. Sci.*, 51 (2009) 1990.
24. S.K. Shukla, M.A. Quraishi, *Corros. Sci.*, 52 (2010) 314.
25. F. Bentiss, M. Traisnel, M. Lagrenee, *Corros. Sci.*, 42 (2000) 127.
26. S.K. Shukla, E.E. Ebenso, *Int. J. Electrochem. Sci.*, 6 (2011) 3277.
27. J.B. Foresman and A. Frisch, *Exploring Chemistry with Electronic Structure Methods*, Gaussian, Inc., Pittsburg, PA (1995) USA.
28. P. Senet, *Chem. Phys. Lett*., 275 (1997) (5-6) 527-532.
29. I. Lukovits, E. Kalman and F. Zucchi, *Corrosion*, 57 (2001) 3.